ScientificScholar®
Knowledge is power
Publisher of Scientific Journals

www.clinicalimagingscience.org

Journal of Clinical Imaging Science

Breast Imaging *Original Research*

Whole-lesion histogram analysis of apparent diffusion coefficient for the assessment of non-mass enhancement lesions on breast MRI

Natsuko Kunimatsu[1], Akira Kunimatsu[2], Yoshihiro Uchida[3], Ichiro Mori[4], Shigeru Kiryu[5]

[1]Department of Radiology, Sanno Hospital, Akasaka, Minato–ku, Tokyo, Japan [2]Department of Radiology, International University of Health and Welfare, Mita Hospital, Minato–ku, Tokyo, Japan, [3]Department of Breast Surgery, Sanno Medical Center, Akasaka, Minato–ku, Tokyo, Japan, [4]Diagnostic Pathology Center, International University of Health and Welfare, Kozunomori 4–3, Narita, Chiba, Japan, [5]Department of Radiology, International University of Health and Welfare, Kozunomori 4–3, Narita, Chiba, Japan.

***Corresponding author:**
Natsuko Kunimatsu,
Department of Radiology, Sanno Hospital, Akasaka, Minato–ku, Tokyo, Japan.

idanatsu3@gmail.com

Received : 08 November 2021
Accepted : 06 March 2022
Published : 22 March 2022

DOI
10.25259/JCIS_201_2021

Quick Response Code:

ABSTRACT

Objectives: To investigate the application of apparent diffusion coefficient (ADC) histogram analysis in differentiating between benign and malignant breast lesions detected as non-mass enhancement on MRI.

Materials and Methods: A retrospective study was conducted for 25 malignant and 26 benign breast lesions showing non-mass enhancement on breast MRI. An experienced radiologist without prior knowledge of the pathological results drew a region of interest (ROI) outlining the periphery of each lesion on the ADC map. A histogram was then made for each lesion. Following a univariate analysis of 18 summary statistics values, we conducted statistical discrimination after hierarchical clustering using Ward's method. A comparison between the malignant and the benign groups was made using multiple logistic regression analysis and the Mann-Whitney *U* test. A *P*-value of less than 0.05 was considered statistically significant.

Results: Univariate analysis for the 18 summary statistics values showed the malignant group had greater entropy ($P < 0.001$) and lower uniformity ($P < 0.001$). While there was no significant difference in mean and skewness values, the malignant group tended to show a lower mean ($P = 0.090$) and a higher skewness ($P = 0.065$). Hierarchical clustering of the 18 summary statistics values identified four values (10th percentile, entropy, skewness, and uniformity) of which the 10th percentile values were significantly lower for the malignant group ($P = 0.035$).

Conclusions: Whole-lesion ADC histogram analysis may be useful for differentiating malignant from benign lesions which show non-mass enhancement on breast MRI.

Keywords: Breast neoplasms, Diffusion magnetic resonance imaging, Histogram analysis, Magnetic resonance imaging, Non-mass enhancement

INTRODUCTION

Magnetic resonance imaging (MRI) has been widely used as an essential tool for detecting suspected breast cancer and determining its extent. The shape, distribution of the lesions, the dynamic contrast enhancement pattern including the kinetic curve have been used for MRI interpretation. According to the terminology of the second edition of the Breast Imaging Reporting and Data System (BI-RADS)—MRI, "non-mass enhancement" is defined as terminology involving distribution and internal enhancement that do not meet criteria for a mass after injecting a contrast medium.[1,2] Regarding the distribution of non-mass enhancement, linear and/or segmental enhancement may indicate malignancy, and the possibility of malignancy is suggested to be high

for ductal enhancement, including linear/branching, clumped, and clustered ring enhancement patterns among internal enhancement.[1,2] Ductal carcinoma in situ (DCIS) mainly corresponds to these non-mass enhancement lesions on breast MRI though several reports suggest that benign preoperative lesions, such as fibrocystic disease, also demonstrate some non-mass enhancement patterns.[3-9] To differentiate enhancement patterns between benign and malignant breast lesions, Tozaki *et al.* reported that segmental distribution, clustered ring enhancement, and branching-ductal pattern enhancement were frequently observed in malignant lesions, while a ductal pattern in benign lesions showed a linear-ductal pattern or stippled punctate enhancement.[5] Despite this increasing knowledge regarding enhancement patterns, we are still not able to confidently distinguish between benign and malignant lesions on MR images.

Apparent diffusion coefficient (ADC) has been established as a diagnostic indicator for various malignant lesions. It represents the flux of water or other small molecules via Brownian motion during a certain period and accommodates the detail of microstructural characteristics. Previous studies have reported the presence of a significant inverse correlation between ADC values and tumor cellularity,[10-12] pathological aggressiveness or malignancy,[13,14] and Ki-67 expression[15] of histological specimens in various neoplasms. Evaluation of ADC values for breast MRI has been also reported.[16-18]

Histogram analysis of ADC has been introduced to assess the heterogeneity of the diffusion distribution of several types of tumors in the body. Previous studies showed that measures of ADC histograms reflect the histopathological heterogeneity, distributions of cellular density, and tissue degeneration.[14,19] Currently, ADC histogram analysis has been used to investigate breast cancer as well.[20-23] Suo *et al.* analyzed breast mass lesions using a whole-lesion ADC histogram and suggested it may facilitate differentiation between benign and malignant lesions at 3.0T MRI.[22] Considering these reported findings, we originally applied a volumetric, whole-lesion ADC histogram analysis for non-mass enhancement shown on breast MRI.

The purpose of this study was to investigate whole-lesion ADC histogram analysis to determine which histogram measures differentiate benign from malignant breast lesions showing non-mass enhancement on MRI.

MATERIALS AND METHODS

Study ethics

This retrospective study was approved by our institutional review board and informed consent was waived.

Subjects

Initially, we searched medical records to identify patients who underwent contrast-enhanced breast MRI for imaging diagnosis of breast lesions on a 3.0T MRI scanner at our institution between February 2014 and August 2019. We identified 1,380 breast MRI studies and reviewed those images and radiological reports. In the 1,380 examinations, 188 lesions showed non-mass enhancement on contrast-enhanced MRI. These BIRADS-MRI based findings were obtained from original radiological diagnosis reports and secondary reviews by one radiologist (N.K.). Of these 188 breast lesions, the final histopathologic diagnosis was confirmed for 51 lesions (25 breast cancer lesions as the malignant group and 26 benign lesions as the benign group), which were enrolled in our analysis. The age of patients ranged from 37–74 years for the malignant group, and 38–54 for the benign group, with a mean age of 52.0 and 45.5 years, respectively. One patient had a benign lesion in both breasts. The average time lapse between MRI and pathological diagnosis was 79 days (range: 0–322 days) for the malignant group and 34 days (0–361 days) for the benign group. Cases of long-time lapses between MRI and pathology were due to follow-up diagnoses with modalities other than MRI for benign lesions, and neoadjuvant chemotherapy for malignant lesions. MRI studies of all cases were done before any treatment. Histopathologic results of the 26 benign lesions were obtained by fine-needle aspiration cytology (one lesion), core needle biopsy (23 lesions), or excisional biopsy (two lesions) all of which showed fibrocystic disease. Of the 25 malignant lesions, 23 were pathologically diagnosed after surgical removal at our institution, and two lesions were diagnosed by core needle biopsy. One of the two malignant lesions underwent core needle biopsy in our institution and surgical removal was done in another hospital. The other malignant lesion was treated by hormonal therapy without surgery in accordance with the patient's wishes. Therefore, 26 benign lesions (fibrocystic disease) are included as the benign group and 25 breast cancer lesions are included as the malignant group in this study.

MRI protocols

MR imaging data were retrieved from the Picture Archiving and Communication System of our institution. All examinations were performed using a 3.0–T unit (Achieva 3T TX, Philips Medical Systems, Best, The Netherlands) with the patients in a prone position using a dedicated breast coil (SENSE–Breast 7 TX). The MRI acquisition protocols were as follows: T2-weighted fat-suppressed imaging (TR/TE, 4095–4838/62–63 ms; slice thickness, 2.2 mm; interslice gap, 0.5 mm; reconstructed voxel size, 0.59 × 0.59 × 5.0 mm, a field of view, 30 cm; acquisition matrix, 420 × 318), diffusion-weighted imaging (TR/TE, 6500/65 ms; slice thickness, 5 mm; interslice gap, 1 mm; acquisition matrix, 92 × 119; 0 and 1,000 s/mm^2 of b values), and coronal, dynamic, fat-suppressed 3D T1-weighted imaging for the bilateral breasts with enhanced T1 high-resolution isotropic volume

excitation (eTHRIVE) (TR/TE, 3.1/1.1 ms; a field of view, 30 cm; slice thickness, 1.0 mm; acquisition matrix, 384 × 288 or 408 × 286; reconstructed voxel size, 0.39 × 0.39 × 1.0 mm), before, 1 minute after, and 8 minutes after a rapid intravenous bolus injection of 0.1 mmol/L gadopentetate dimeglumine (Magnevist, Bayer Healthcare Pharmaceuticals, Montville, NJ, USA) per kilogram body weight. A postcontrast sagittal 3D T1-weighted turbo field echo imaging with fat-suppression for the bilateral breasts (TR/TE, 3.1–4.0/1.1–2.1 ms; a field of view, 22 cm; slice thickness, 0.8 mm; acquisition matrix, 288 × 259; reconstructed voxel size, 0.43 × 0.43 × 0.8 mm) was also acquired at approximately 4 minutes (right breast) and 6 minutes (left breast) after intravenous injection of contrast media. MR images were obtained irrespective of the patients' menstrual cycles.

Image analysis

We used image data processing software (ITK-SNAP 3.8.0., Penn Image Computing & Science Laboratory, the University of Pennsylvania, http://www.itksnap.org/pmwiki/pmwiki.php) for the image data analysis, with which image registration was performed for ADC maps and contrast-enhanced MR images to align them on the monitor. Each region of interest (ROI) was carefully drawn by an experienced radiologist who did not know the pathological diagnoses, such that the ROI outlined the periphery of lesions on the ADC map, referencing contrast-enhanced MR images obtained 8 minutes after injection of the contrast media. The manually-drawn ROI on an ADC map was simultaneously displayed on other 3-dimensional ADC maps and contrast-enhanced MRI in multiplanar (axial, sagittal, and coronal) views [Figure 1]. Then, first-order histogram statistics were calculated for each lesion using open-source software (PyRadiomics 2.1.0., pyradiomics community, https://pyradiomics.readthedocs.io/en/latest/).

Statistical analyses

We performed a nonparametric Mann-Whitney *U* test with Bonferroni correction for univariate analysis for 18 summary statistic values (10th percentile, 90th percentile, energy, entropy, interquartile range, kurtosis, maximum, mean absolute deviation, mean, median, minimum, range, robust mean absolute deviation, root mean squared, skewness, total energy, uniformity, and variance) to assess the differences between benign and malignant groups. We then chose four variable values (10th percentile, entropy, skewness, and uniformity) from these 18 statistic values after hierarchical clustering using Ward's method; and developed a model with multiple logistic regression. For these statistical analyses, we used R {R Core Team (2016). R: A language and environment for statistical computing. R Foundation for Statistical Computing, Vienna, Austria. https://www.R-project.org/}. A *P*-value of less than 0.05 was considered statistically significant.

RESULTS

The 25 lesions of the malignant group diagnosed as breast cancer included DCIS (three lesions), invasive ductal cancer with predominant intraductal component (two lesions), invasive lobular cancer (one lesion), and invasive ductal cancer (19 lesions). The 26 lesions of the benign group were all diagnosed as fibrocystic disease, which is primarily characterized by adenosis including sclerosing adenosis and ductal hyperplasia.

Results of the univariate analysis for the 18 summary statistic values showed that the malignant group had greater entropy ($P < 0.001$) [Figure 2a] and lower uniformity ($P < 0.001$) [Figure 2b] than the benign group. Though there were no significant differences in the mean and skewness, the malignant group tended toward a low mean value ($P = 0.090$) [Figure 2c] and tended toward a higher skewness value ($P = 0.0646$) [Figure 2d].

The dendrogram of the hierarchical clustering is shown in [Figure 3]. Of the four values (10th percentile, entropy, skewness, and uniformity) selected from the 18 statistic values, the 10th percentile value was significantly lower for the malignant group ($P = 0.035$) [Figure 4]. The relative risk was 0.996 (95% confidence interval: 0.993–0.999).

DISCUSSION

We investigated ADC histograms of lesions showing non-mass enhancement on breast MRI to analyze differences between benign and malignant lesions. Univariate analysis

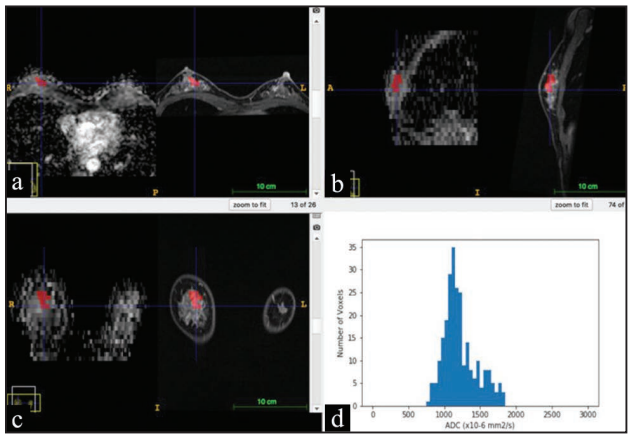

Figure 1: Multiplanar reconstruction of ADC map and contrast-enhanced MRI of a breast lesion (diagnosed as fibrocystic disease by core needle biopsy). A region of interest (ROI) manually drawn on an ADC map and displayed corresponding sites on contrast-enhanced MRI by using the image registration. Red-colored ROIs show the breast lesion in 3-dimensional views: (a), axial views of the ADC map (left side) and contrast-enhanced MRI (right side); (b), sagittal views of the ADC map (left side) and contrast-enhanced MRI (right side); (c), coronal views of the ADC map (left side) and contrast-enhanced MRI (right side); and (d), an ADC histogram calculated for the red-colored ROI.

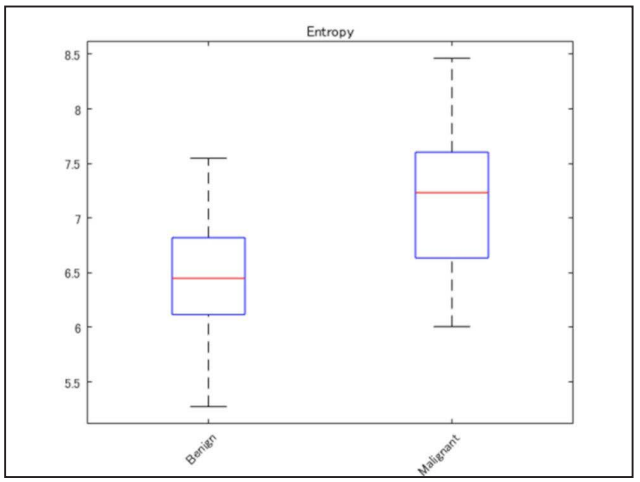

Figure 2a: Box plots of entropy. At the univariate analysis, the malignant group had greater entropy ($P < 0.001$) than the benign group.

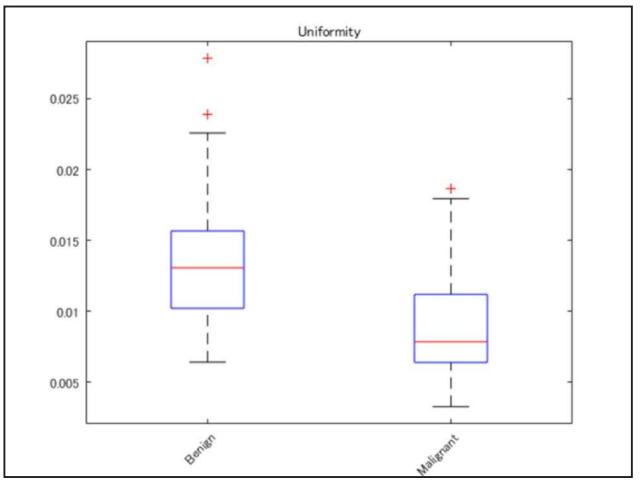

Figure 2b: Box plots of uniformity. The malignant group had lower uniformity ($P < 0.001$) than the benign group. Red plus symbols indicate outliers.

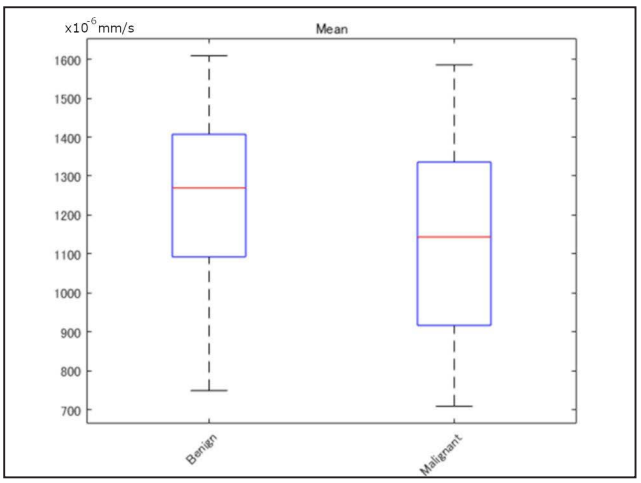

Figure 2c: Box plots of mean. Though there was no significant difference, the mean of the malignant group tends to show lower values ($P = 0.090$).

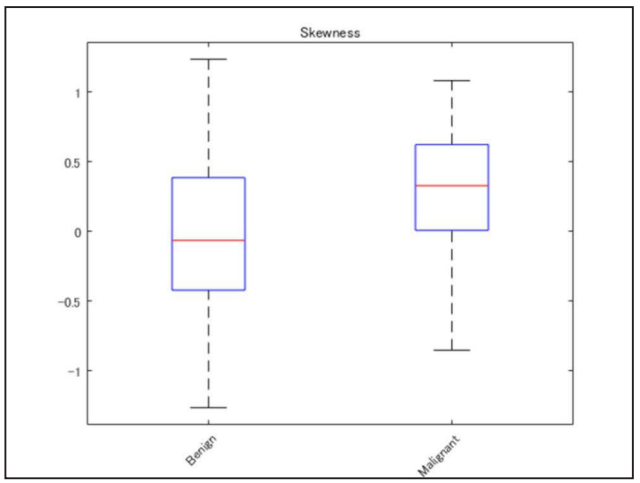

Figure 2d: Box plots of skewness. Skewness of the malignant groups tends to show higher values ($P = 0.646$) than the benign group.

showed greater entropy ($P < 0.001$) and lower uniformity ($P < 0.001$) for the malignant group compared to the benign group. Multiple logistic regression analysis of four summary statistic values identified by hierarchial clustering showed a significantly lower 10th percentile value for the malignant group ($P = 0.035$).

We consider that the greater entropy and lower uniformity of the malignant lesion group may be due to pathological heterogeneity and nonuniform diffusivity of malignant tissues in the lesion. The low 10th percentile values of the malignant group may represent the limitation of diffusivity caused by high cellular density.

While there was no significant difference in the mean and skewness, the tendencies of lower mean ($P = 0.090$) and higher skewness ($P = 0.0646$) of the malignant group suggest malignant lesions on average have low diffusion limits and show a positively skewed distribution as analyzed based on ADC values.

Non-mass enhancement on the contrast-enhanced MRI can be observed for both benign and malignant lesions, including DCIS, minimal invasive ductal cancer, invasive lobular cancer, high-risk lesions like atypical ductal cancer, and fibrocystic disease.[2-9] As for morphological patterns, the presence of segmental or linear distribution,

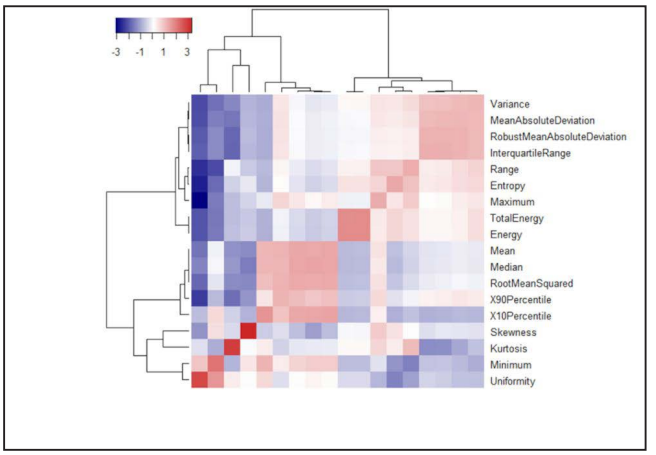

Figure 3: A double dendrogram showing the hierarchical clustering results. Of the 18 summary statistics values shown by rows, four values (10th percentile, entropy, skewness, and uniformity) were selected after hierarchical clustering using Ward's method. The numbers of the scale bar are z-scores, with dark red representing high values and dark blue representing low values.

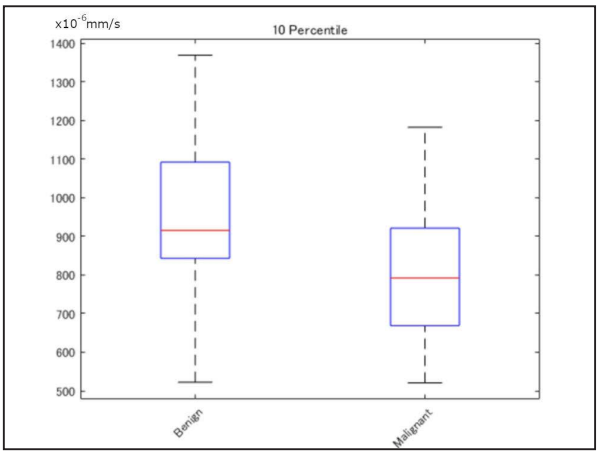

Figure 4: Box plots of the 10 percentile values. At the multiple logistic regression analysis, the 10th percentile values were significantly lower in the malignant group ($P = 0.035$). The relative risk was 0.996 (95% confidence interval).

or clustered ring enhancement is a frequent manifestation of DCIS on dynamic MRI[2-9] though they are sometimes difficult to differentiate.

Differences in ADC values of MRI between benign and malignant breast lesions have been reported.[16,18] Histogram analysis of ADC has been recently used to investigate optimal indices for differentiation between benign and malignant lesions of the breast.[23]

There are several reports of DCIS on MRI detected as a non-mass enhancement lesion and exhibits segmental or ductal distribution and clumped internal architecture.[2-9,17,23] However, clinical diagnosis may be problematic because DCIS or minimal invasive ductal cancer, invasive lobular cancer, high-risk lesions like atypical ductal cancer, or fibrocystic disease may also show non-mass enhancement on contrast-enhanced MRI.[2,3,7,8,23] With dynamic MRI of non-mass enhancement lesions, segmental, linear distribution, and clustered ring enhancement are frequent manifestations of DCIS.[4,5] ADC can be a diagnostic indicator based on the water diffusion restrictions in combination with morphological evaluation of contrast-enhanced MRI.

Yabuuchi *et al.* reported that segmental distribution, clumped internal enhancement, and a mean ADC value of less than 1.3×10^{-3} mm^2/s were the strongest indicators of malignancy among lesions showing non-mass enhancement on contrast-enhanced breast MR images.[7] Suo *et al.* investigated the utility of whole-lesion ADC histogram analysis for mass lesions in the breast, reporting that the mean, minimum, maximum, and 10th/25th/50th/75th/90th percentile ADCs were significantly lower, while skewness, and entropy ADCs were significantly higher in malignant lesions compared with benign lesions.[22] Park *et al.* previously reported that ADC of invasive ductal cancer showed significantly lower values compared with those of DCIS with a threshold of 1.185×10^{-3} mm^2/s.[23] However, to our knowledge, there has been no previous study that conducted a volumetric, whole-lesion, histogram analysis of breast lesions showing non-mass enhancement.

In this study, we investigated whole-lesion ADC histogram analyses for non-mass enhancement lesions of the breast MRI, and report on the statistical differences between malignant and benign lesions, which we believe to be a new finding that may help in the diagnosis of non-mass enhancement lesions of the breast.

Our study had several limitations. First, this was a retrospective study. Since lesions showing non-mass enhancement likely fall under the category of careful follow-up observation, a resection or biopsy of the lesion is less frequently performed than for those showing a solid mass on MRI. A second limitation is the small number of subjects included in this study. Third, this retrospective study was conducted using one MRI machine at a single institution, though the MRI data collection method was considered uniform and reliable. The measurement of ADC values depends on the parameters of each MRI unit, thus further study using a variety of MRI machines will lead to a more robust definition for ADC-based diagnosis. Fourth, the ROIs for individual lesions on the ADC map were manually drawn by a radiologist while referring to contrast-enhanced MRI in multiplanar views using an image registration function. Due to lower spatial resolution and inherent distortion of ADC maps, compared with contrast-enhanced MRI, the location and shape of the breast lesion may not have been identical between the ADC maps and contrast-enhanced images. A careful comparison of these two is required when setting an ROI for each lesion.

In conclusion, our investigation of whole-lesion ADC histogram analysis of non-mass enhancement on breast MRI suggests its potential for possible use in differentiating between benign and malignant lesions.

Acknowledgment

This work was supported by JSPS KAKENHI Grant Number JP18K07629.

Declaration of patient consent

Institutional Review Board (IRB) permission was obtained for the study.

Financial support and sponsorship

Nil.

Conflicts of interest

There are no conflicts of interest.

REFERENCES

1. Morris EA, Comstock C, Lee C. BIRADS-MRI-5th-Edition.PDF. file:///Users/sanjeeva/Downloads/BIRADS-MRI-5th-EditionPDF [Internet]. 2013;533. Available from:http://nld.by/omr/breast/BI-RADS/BIRADS-MRI-5th-Edition.PDF
2. Milosevic ZC. BI-RADS-MRI terminology and evaluation of intraductal carcinoma and ductal carcinoma in situ. Breast Cancer 2013;20:13–20.
3. Liberman L, Morris EA, Dershaw DD, Abramson AF, Tan LK. Ductal enhancement on MR imaging of the breast. Am J Roentgenol 2003;181:519–25.
4. Morakkabati-Spitz N, Leutner C, Schild H, Traeber F, Kuhl C. Diagnostic usefulness of segmental and linear enhancement in dynamic breast MRI. Eur Radiol 2005;15:2010–7.
5. Tozaki M, Fukuda K. High-spatial-resolution MRI of non-masslike breast lesions: Interpretation model based on BI-RADS MRI descriptors. Am J Roentgenol 2006;187:330–7.
6. Kuhl CK, Schrading S, Bieling HB, Wardelmann E, Leutner CC, Koenig R, *et al.* MRI for diagnosis of pure ductal carcinoma in situ: a prospective observational study. Lancet 2007;370:485–92.
7. Yabuuchi H, Matsuo Y, Kamitani T, Setoguchi T, Okafuji T, Soeda H, *et al.* Non-mass-like enhancement on contrast-enhanced breast MR imaging: Lesion characterization using combination of dynamic contrast-enhanced and diffusion-weighted MR images. Eur J Radiol 2010;75:e126–e32.
8. Chadashvili T, Ghosh E, Fein-Zachary V, Mehta TS, Venkataraman S, Dialani V, *et al.* Nonmass enhancement on breast MRI: Review of patterns with radiologie-pathologie correlation and discussion of management. Am J Roentgenol 2015;204:219–27.
9. Milosevic ZC, Nadrljanski MM, Milovanovic ZM, Gusic NZ, Vucicevic SS, Radulovic OS. Breast dynamic contrast enhanced MRI: Fibrocystic changes presenting as a non-mass enhancement mimicking malignancy. Radiol Oncol 2017; 51:130–6.
10. Manenti G, Di Roma M, Mancino S, Bartolucci D a, Palmieri G, Mastrangeli R, *et al.* Malignant renal neoplasms: correlation between ADC values and cellularity in diffusion weighted magnetic resonance imaging at 3 T. Radiol Med 2008;113:199–213.
11. Gibbs P, Liney GP, Pickles MD, Zelhof B, Rodrigues G, Turnbull LW. Correlation of ADC and T2 measurements with cell density in prostate cancer at 3.0 Tesla. Invest Radiol 2009;44:572–6.
12. Surov A, Meyer HJ, Wienke A. Correlation between apparent diffusion coefficient (ADC) and cellularity is different in several tumors: a meta-analysis. Oncotarget 2017;8:59492–9.
13. Bollineni VR, Kramer G, Liu Y, Melidis C, deSouza NM. A literature review of the association between diffusion-weighted MRI derived apparent diffusion coefficient and tumour aggressiveness in pelvic cancer. Cancer Treatment Reviews 2015;41:496–502.
14. Mimura R, Kato F, Tha KK, Kudo K, Konno Y, Oyama-Manabe N, *et al.* Comparison between borderline ovarian tumors and carcinomas using semi-automated histogram analysis of diffusion-weighted imaging: Focusing on solid components. Jpn J Radiol 2016;34:229–37.
15. Surov A, Meyer HJ, Wienke A. Associations between apparent diffusion coefficient (ADC) and KI 67 in different tumors: A meta-analysis. Part 1: ADCmean. Oncotarget 2017;8:75434–44.
16. Kinoshita T, Yashiro N, Ihara N, Funatu H, Fukuma E, Narita M. Diffusion-weighted half-fourier single-shot turbo spin echo imaging in breast tumors: Differentiation of invasive ductal carcinoma from fibroadenoma. J Comput Assist Tomogr 2002;26:1042–6.
17. Tozaki M, Fukuma E. 1H MR spectroscopy and diffusion-weighted imaging of the breast: Are they useful tools for characterizing breast lesions before biopsy? Am J Roentgenol 2009; 193:840–9.
18. Palle L, Reddy B. Role of diffusion MRI in characterizing benign and malignant breast lesions. Indian J Radiol Imaging 2009;19:287–90.
19. Kunimatsu N, Kunimatsu A, Miura K, Mori I, Nawano S. Differentiation between solitary fibrous tumors and schwannomas of the head and neck: An apparent diffusion coefficient histogram analysis. Dentomaxillofacial Radiol 2019;48:20180298.
20. Kim EJ, Kim SH, Park GE, Kang BJ, Song BJ, Kim YJ, *et al.* Histogram analysis of apparent diffusion coefficient at 3.0T: Correlation with prognostic factors and subtypes of invasive ductal carcinoma.J Magn Reson Imaging 2015;42:1666–78.
21. Kim YJ, Kim SH, Lee AW, Jin M-S, Kang BJ, Song BJ. Histogram analysis of apparent diffusion coefficients after neoadjuvant chemotherapy in breast cancer. Jpn J Radiol 2016;34:657–66.
22. Suo S, Zhang K, Cao M, Suo X, Hua J, Geng X, *et al.* Characterization of breast masses as benign or malignant at 3.0T MRI with whole-lesion histogram analysis of the apparent diffusion coefficient. J Magn Reson Imaging 2016;43:894–902.
23. Park GE, Kim SH, Kim EJ, Kang BJ, Park MS. Histogram analysis of volume-based apparent diffusion coefficient in breast cancer. Acta radiol 2017;58:1294–302.

How to cite this article: Kunimatsu N, Kunimatsu A, Uchida Y, Mori I, Kiryu S. Whole-lesion histogram analysis of apparent diffusion coefficient for the assessment of non-mass enhancement lesions on breast MRI. J Clin Imaging Sci 2022;12:12.